Supporting Information

Hong et al. 10.1073/pnas.1324012111

SI Methods

Channel Mutants. Expression of Hv1 mutants with alanine substitutions at positions 109, 150, 178, 181, and 182 provided strong proton currents similar in size to the WT channel (Fig. 2*B*). We mutated R211 to serine, because the substitution was previously shown to be well-tolerated by the protein (1). Neutralizing mutations of charged residues D112 and R208 proved to be highly perturbative, which was previously reported (2, 3). Currents measured from any of the alanine-, asparagine-, or glutamine-substituted channels at these positions were too small for reliable measurement of inhibition. However, conservative substitutions D112E, and R208K produced functioning channels, with current levels comparable with WT.

Mutant Cycle Analysis. In mutant cycle analysis, mutations that cause large changes in K_d of related compounds do not necessarily produce large $\Delta\Delta G^o$ values. Only mutations that cause different changes in channel affinity for related compounds can produce large $\Delta\Delta G^o$ values (Fig. S1). Mutations that alter binding affinity by long-range perturbations, such as overall backbone structure of a helix, are more likely to produce generalized effects on binding rather than selective effects on individual inhibitors. If a mutation produces the same change in K_d for all of the related compounds, all of the $\Delta\Delta G^o$ values associated with it will be ~0. As a result, the mutated residue cannot be confirmed to be part of the binding site. This reduces the occurrence of false positives. However, it does not completely eliminate the possibility.

1. Berger TK, Isacoff EY (2011) The pore of the voltage-gated proton channel. *Neuron* 72(6):991–1000.
2. Musset B, et al. (2011) Aspartate 112 is the selectivity filter of the human voltage-gated proton channel. *Nature* 480(7376):273–277.
3. Kulleperuma K, et al. (2013) Construction and validation of a homology model of the human voltage-gated proton channel hHV1. *J Gen Physiol* 141(4):445–465.

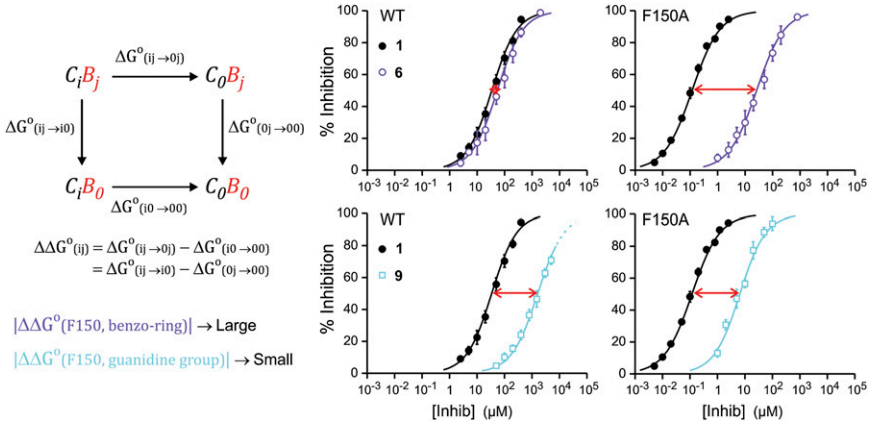

Fig. S1. Examples of mutant cycle analysis applied to position F150. Red arrows indicate the separations between the inhibition curves for modified and unmodified inhibitor. When the separation in the mutant channel is different from the separation in the WT channel, $|\Delta\Delta G^o|$ is larger than zero. In the case of compound 6, the difference in separation is large, and therefore, $|\Delta\Delta G^o|$ is large. This result is considered indicative of an interaction between F150 and the benzo ring of the inhibitor (modified in compound 6). In the case of compound 9, the difference in separation is negligible, and therefore, $|\Delta\Delta G^o|$ is negligible. This result indicates that F150 does not interact with the guanidine group of the inhibitor (modified in compound 9). B_j, inhibitor with unmodified benzo ring or guanidine group; B_0, inhibitor with modified benzo ring (compound 6) or modified guanidine group (compound 9); C_i, Hv1 F150; C_0, Hv1 F150A. Fig. 3*A* has additional details.

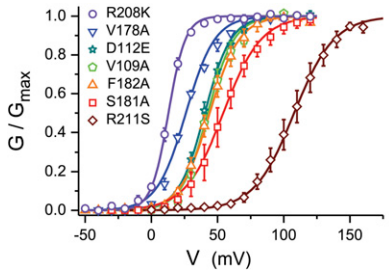

	$V_{1/2}$ (mV)	Slope (mV)
V109A	42.6 ± 1.7	10.0 ± 1.0
D112E	40.4 ± 1.9	9.9 ± 0.3
F150A	29.0 ± 2.8	10.7 ± 0.3
E153C	-1.6 ± 3.6	11.4 ± 1.3
V178A	26.1 ± 0.8	11.2 ± 1.1
S181A	52.7 ± 4.8	12.5 ± 1.7
F182A	44.0 ± 2.8	11.2 ± 1.0
R208K	12.9 ± 0.9	6.5 ± 0.4
R211S	107.9 ± 4.6	15.1 ± 2.2
WT	53.1 ± 2.3	10.9 ± 0.8

Fig. S2. Voltage dependence of activation of Hv1 channels tested for inhibition by guanidine derivatives. Conductance vs. voltage relationships were determined as previously described (1) from proton currents recorded in inside-out patches. $pH_o = pH_i = 6.0$. Error bars are SEM ($n \geq 4$). Curved lines are Boltzmann fits of the data. Fit parameters are reported in *Right*. $V_{1/2}$ and slope values for mutants F150A and E153C and Hv1 WT are from previously published works (1, 2) and provided here as reference (gray).

1. Tombola F, Ulbrich MH, Kohout SC, Isacoff EY (2010) The opening of the two pores of the Hv1 voltage-gated proton channel is tuned by cooperativity. *Nat Struct Mol Biol* 17(1):44–50.
2. Hong L, Pathak MM, Kim IH, Ta D, Tombola F (2013) Voltage-sensing domain of voltage-gated proton channel Hv1 shares mechanism of block with pore domains. *Neuron* 77(2): 274–287.

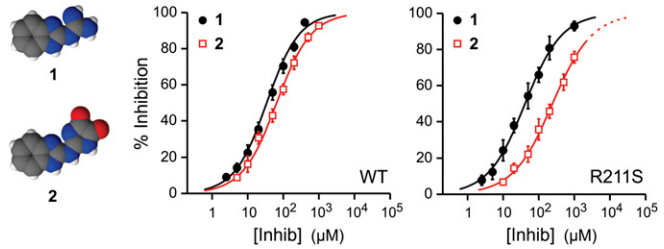

Fig. S3. Interaction between the guanidine group of 2-guanidinobenzimidazole (2GBI) and R211 probed with compound 2. Dose–response curves for the inhibition of Hv1 WT and R211S produced by the indicated compounds. Each point represents the average inhibition from three to six measurements ± SD. Curved lines are Hill fits. Fit parameters for compound 1 are reported in Table S1. Fit parameters for compound 2 are $K_d = 65.1 \pm 3.2$ μM and $h = 0.89 \pm 0.03$ for WT and $K_d = 244 \pm 12$ μM and $h = 0.78 \pm 0.03$ for R211S. The dotted line in *Right* represents extrapolation into a concentration range where compound 2 has low solubility. The coupling free energy value for R211 and the guanidine group of the inhibitor was 2.79 ± 0.28 kJ/mol ($\Delta\Delta G^o/\Delta G^o_b = -11.0 \pm 1.1\%$).

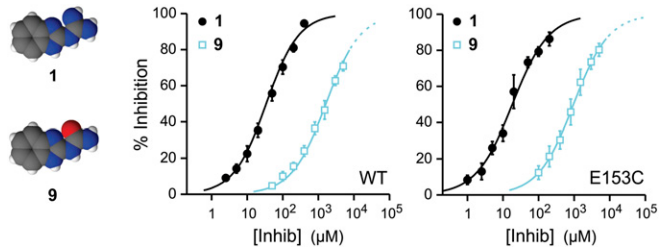

Fig. S4. Lack of interaction between the guanidine group of 2GBI and E153 probed with compound 9. Dose–response curves for the inhibition of Hv1 WT and E153C produced by the indicated compounds. Each point represents the average inhibition from three to eight measurements ± SD. Curved lines are Hill fits. Fit parameters for Hv1 WT are reported in Table S1. Fit parameters for E153C are $K_d = 18.2 \pm 1.2$ μM and $h = 0.85 \pm 0.04$ for compound 1 and $K_d = 955 \pm 26$ μM and $h = 0.87 \pm 0.02$ for compound 9. Dotted lines represent extrapolation into a concentration range where compound 9 has low solubility. The coupling free energy value for E153 and the guanidine group of the inhibitor was 0.23 ± 0.29 kJ/mol ($\Delta\Delta G^o/\Delta G^o_b = -0.9 \pm 1.1\%$).

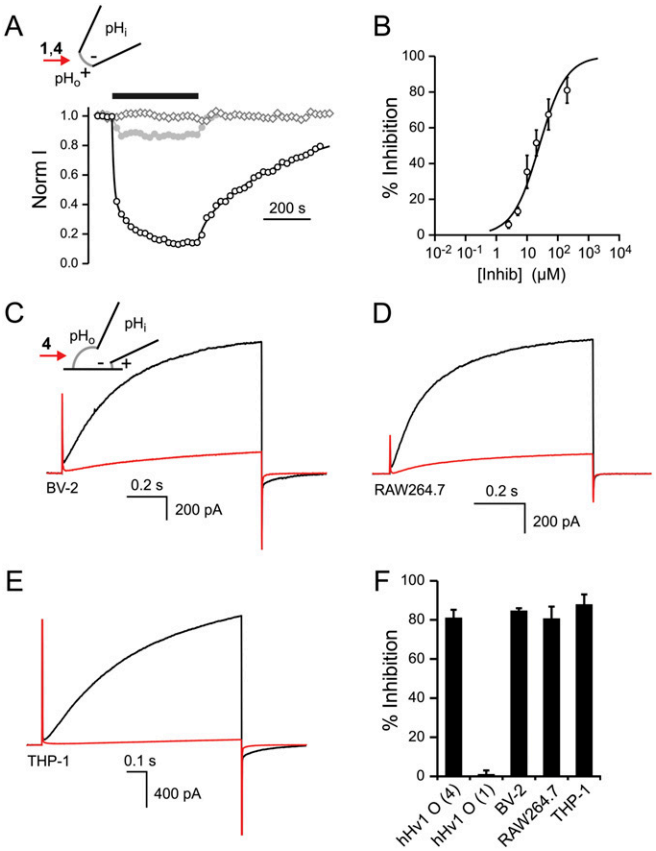

Fig. S5. Inhibition of recombinant and native proton channels by a membrane-permanent 2GBI analog. (*A*) Time courses of Hv1 inhibition by compounds 1 (2GBI) and 4 (ClGBI) added to the extracellular side of the membrane. Proton currents were measured in outside-out patches from oocytes expressing human Hv1 on depolarization to +120 mV from a holding potential of −80 mV. pH_i was 6.0, and pH_o was 7.5. Horizontal black bar indicates the presence of 200 μM inhibitor in the bath solution (gray open diamonds, 200 μM 2GBI; gray filled circles, 5 μM ClGBI; black open circles, 200 μM ClGBI). Points were fitted by exponential functions for inhibition and recovery (black curves; in the text). (*B*) Dose–response curve of Hv1 inhibition by extracellular ClGBI. Reductions in proton current were measured as a function of inhibitor concentration in outside-out patches as in *A*. Each point represents the average inhibition from three to four measurements ± SD. Black curve is the Hill fit. Parameters are in the text. (*C*–*E*) Effect of extracellular ClGBI on native proton currents measured in microglial BV-2 cells and monocyte/macrophage cells RAW264.7 and THP-1. Whole-cell currents were recorded in the absence (black) and presence (red) of 200 μM ClGBI in the bath under the same conditions used in *A*. (*F*) Quantification of proton channel inhibition by extracellular ClGBI (200 μM). The effect of the same concentration of extracellular 2GBI on Hv1 currents measured in oocytes (O) is provided for comparison. Bars are averages ± SEM ($n \geq 3$).

Table S1. Fit parameters for dose–response curves shown in Fig. 3*A*

	1		4		6		8		9		11	
Channel	K_d (μM)	h	K_d (μM)	h	K_d (μM)	h	K_d (μM)	h	K_d (μM)	h	K_d (μM)	h
WT	34.3 ± 2.5	0.95 ± 0.05	1.55 ± 0.07	0.96 ± 0.04	54.3 ± 3.7	0.93 ± 0.04	62.3 ± 2.4	1.02 ± 0.03	1,630 ± 99	0.90 ± 0.03	7,400 ± 1,200	1.00 ± 0.13
V109A	22.1 ± 1.6	0.90 ± 0.03	1.20 ± 0.10	0.90 ± 0.06	46.1 ± 1.9	0.93 ± 0.02	28.5 ± 1.7	0.87 ± 0.03	1,230 ± 82	0.77 ± 0.05	3,280 ± 230	0.93 ± 0.04
D112E	191 ± 8	1.03 ± 0.03	13.9 ± 0.9	0.99 ± 0.05	148 ± 5	0.92 ± 0.02	230 ± 9	0.89 ± 0.03	5,800 ± 290	0.90 ± 0.04	3,900 ± 650	1.00 ± 0.19
F150A	0.118 ± 0.007	0.86 ± 0.03	0.061 ± 0.003	1.00 ± 0.03	26.3 ± 2.2	0.86 ± 0.04	0.126 ± 0.005	0.87 ± 0.02	6.5 ± 0.6	0.92 ± 0.07	16.5 ± 1.1	0.94 ± 0.04
V178A	13.14 ± 0.39	0.81 ± 0.02	0.660 ± 0.046	0.90 ± 0.04	30.2 ± 4.2	0.84 ± 0.07	22.5 ± 0.6	0.95 ± 0.02	694 ± 16	0.76 ± 0.01	2,500 ± 150	0.80 ± 0.04
S181A	51.9 ± 2.4	0.87 ± 0.03	3.16 ± 0.24	1.04 ± 0.06	71 ± 5	0.80 ± 0.03	104 ± 8	0.98 ± 0.05	2,500 ± 120	0.77 ± 0.02	2,520 ± 200	1.00 ± 0.07
F182A	23.8 ± 1.9	0.93 ± 0.04	1.41 ± 0.11	0.96 ± 0.05	29.8 ± 1.4	0.85 ± 0.03	33.5 ± 1.7	0.96 ± 0.03	1,240 ± 130	0.82 ± 0.06	2,580 ± 290	0.94 ± 0.09
R208K	33.6 ± 1.3	0.84 ± 0.02	2.05 ± 0.16	0.99 ± 0.05	47.2 ± 0.9	0.90 ± 0.01	59.2 ± 2.6	1.02 ± 0.03	1,900 ± 310	0.90 ± 0.11	6,100 ± 2,700	1.00 ± 0.25
R211S	41.3 ± 2.1	0.84 ± 0.03	2.09 ± 0.11	0.97 ± 0.03	188 ± 12	0.85 ± 0.03	57.8 ± 3.9	0.96 ± 0.04	5,600 ± 260	0.94 ± 0.03	1,330 ± 80	1.00 ± 0.06

Table S2. Coupling free energy values for the indicated combinations of channel mutations and inhibitor modifications expressed as percentage of the apparent free energy of binding of 2GBI to Hv1 WT

	$\Delta\Delta G^o/\Delta G^o_b$ (%)				
Channel	4	6	8	9	11
V109A	−1.7 ± 1.2	−2.6 ± 1.3	3.4 ± 1.2	−1.5 ± 1.3	3.6 ± 1.9
D112E	−4.6 ± 1.1	6.9 ± 1.1	4.0 ± 1.0	4.3 ± 1.1	22.9 ± 2.4*
F150A	−23.7 ± 1.1*	−48.1 ± 1.4*	5.2 ± 1.0	−1.4 ± 1.4	4.2 ± 1.9
V178A	−1.0 ± 1.1	−3.6 ± 1.7	0.6 ± 0.9	−1.0 ± 1.0	1.2 ± 1.8
S181A	−2.9 ± 1.2	1.5 ± 1.3	−0.9 ± 1.2	−0.1 ± 1.1	14.5 ± 1.9*
F182A	−2.7 ± 1.4	2.3 ± 1.3	2.5 ± 1.2	−0.9 ± 1.6	6.7 ± 2.1
R208K	−2.9 ± 1.2	1.2 ± 1.0	0.3 ± 1.0	−1.5 ± 1.9	1.7 ± 4.6
R211S	−1.1 ± 1.1	−10.3 ± 1.2*	2.6 ± 1.1	−10.2 ± 1.1*	18.5 ± 1.9*

*Values above threshold.

Table S3. Highest tested concentrations for the indicated compounds and relative percentages of channel inhibition

Channel	$[\mathbf{1}]_{max}$ (mM)	$\%_{inhib}$	$[\mathbf{4}]_{max}$ (mM)	$\%_{inhib}$	$[\mathbf{6}]_{max}$ (mM)	$\%_{inhib}$	$[\mathbf{8}]_{max}$ (mM)	$\%_{inhib}$	$[\mathbf{9}]_{max}$ (mM)	$\%_{inhib}$	$[\mathbf{11}]_{max}$ (mM)	$\%_{inhib}$
WT	0.4	94.5 ± 1.4	0.02	93.6 ± 1.1	2	98.7 ± 0.6	2	97.3 ± 1.2	5	70.8 ± 2.6	4	36.6 ± 4.4
V109A	1	97.7 ± 0.6	0.05	98.7 ± 0.6	0.8	93.7 ± 1.5	2	98.0 ± 1.0	5	77.7 ± 2.8	4	54 ± 6
D112E	2	91.2 ± 2.6	0.2	94.0 ± 3.6	4	95.7 ± 2.5	4	90.7 ± 0.6	5	46 ± 8	4	50.7 ± 4.8
F150A	0.0025	94.5 ± 1.3	0.001	96.0 ± 1.1	0.8	96.0 ± 1.0	0.005	96.7 ± 3.2	0.1	94.0 ± 4.2	0.2	92.7 ± 1.7
V178A	0.5	95.7 ± 2.5	0.02	96.7 ± 1.5	1	98.0 ± 1.7	1	97.3 ± 2.1	5	81.7 ± 2.1	4	59 ± 7
S181A	1	94.5 ± 3.1	0.05	94.5 ± 3.1	2	96.8 ± 2.1	4	94.0 ± 2.6	5	64 ± 6	4	62.3 ± 4.2
F182A	1	97.0 ± 2.6	0.02	95.0 ± 2.9	2	98.0 ± 1.0	2	96.7 ± 4.0	5	79.5 ± 3.3	4	63.1 ± 3.9
R208K	1	95.8 ± 1.7	0.05	97.3 ± 1.5	2	96.3 ± 1.0	2	95.8 ± 3.2	5	70.6 ± 4.6	4	45 ± 9
R211S	1	93.0 ± 2.6	0.05	95.0 ± 2.6	4	93.3 ± 1.2	2	93.7 ± 3.8	5	48 ± 6	4	77 ± 1.6